Supplemental information for "Crystalline solid retains memory of anisotropy in precursor liquid crystalline phase"

Kushal Bagchi[a], Tadej Emeršič[a], Zhongyang Wang[a], Wen Chen[a], Mincheol Kim[a], Christopher Eom[a], Zhang Jiang[b], Joseph Strzalka[b], Juan J de Pablo[a,c], and Paul F Nealey[a,c*]

[a]Pritzker School of Molecular Engineering, The University of Chicago, Chicago, Illinois 60637

[b]X-ray Science Division, Argonne National Laboratory, Lemont, Illinois 60439, United States

[c]Materials Science Division, Argonne National Laboratory, Lemont, Illinois 60439, USA

AUTHOR INFORMATION

Corresponding Author: Paul F Nealey

*Correspondence to: Paul F Nealey

Email: nealey@uchicago.edu

i. AFM linecuts of gratings before and after filling

Linecuts of the AFM images shown in the main text are plotted below. The linecuts support the conclusion that HAT6 partially fills the trenches and grows selectively on the silicon regions.

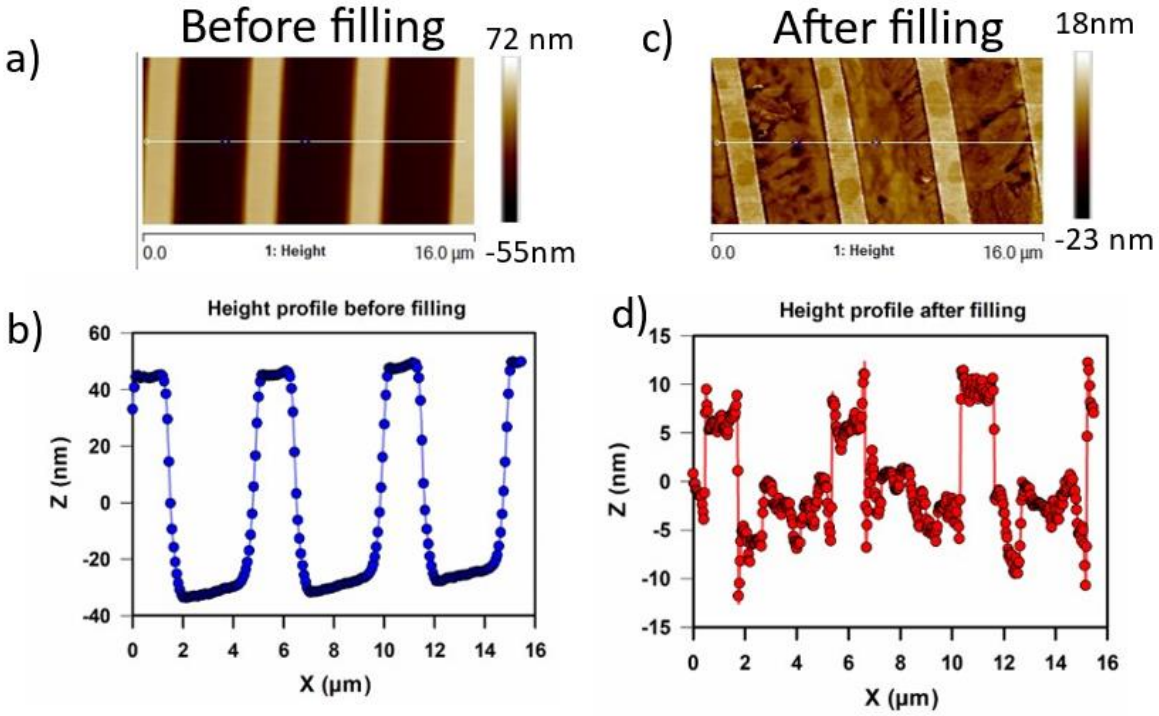

Figure S1: Topography before and after filling microchannels. AFM images and linecuts of topographical X-PS patterns on silicon before (a and b) and after (c and d) filling with HAT6.

ii. Morphology on un-patterned silicon

POM images of a 90 nm thick HAT6 film on un-patterned silicon are shown below in the plastic and liquid crystal states. As the films are polycrystalline, a granular morphology is observed in the POM images.

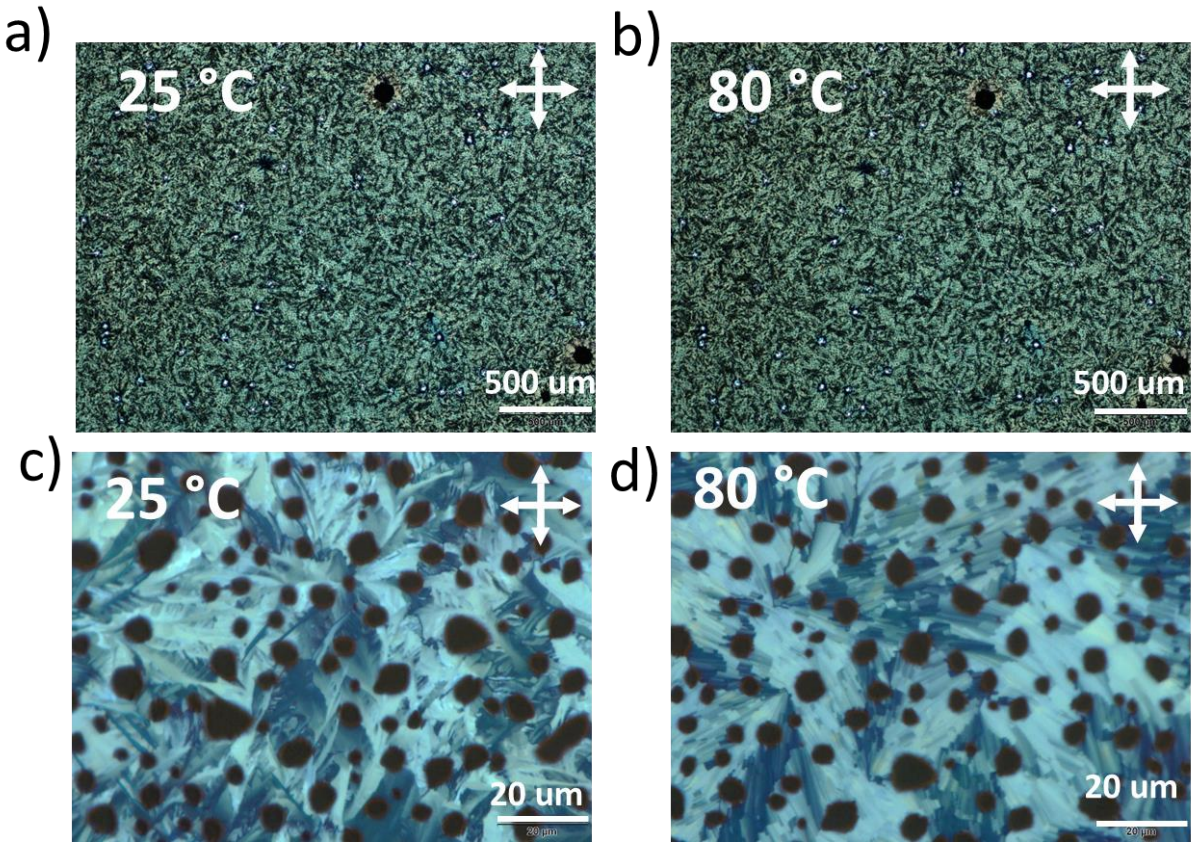

Figure S2: POM images of a 90 nm thick HAT6 film on un-patterned silicon. Images are collected at 25 °C (a and c) and 80 °C (b and d). At 25°C and 80 °C HAT6 is in its plastic and liquid crystal states, respectively. Images a and b are collected with 4X magnification and c and d are acquired at 100X magnification.

iii. Influence of sidewall and substrate chemistry on grapho-epitaxy

To determine the influence of interfacial chemistry on grapho-epitaxy, topological patterns are fabricated wherein the sidewalls and substrates are composed of different materials. Shown in **Figure S3** are POM images of biaxial HAT6 crystals grown in microchannels consisting of silicon (a and b) and X-PS (c and d) sidewalls. For both samples, the microchannels are fabricated on silicon substrates. As shown in **Table S1**, the degree of biaxial alignment is quantitatively similar in microchannels where the sidewalls are composed of silicon and X-PS. We also functionalize the silicon substrate with the silane DMOAP (Dimethyloctadecyl [3-(trimethoxysilyl)propyl]ammonium chloride). The sidewalls are made of gold in the pattern where the substrate is silanized. This ensures that DMOAP grafts only to the substrate and not the side walls. In comparing the right (a,b) and leftmost (e,f) set of images in **Figure S3** we are comparing samples where both the chemistry of the sidewalls and the substrate are varied. Despite the variations of sidewall and substrate chemistry, the degree of alignment of HAT6 crystals in microchannels, quantified in **Table S1**, is similar.

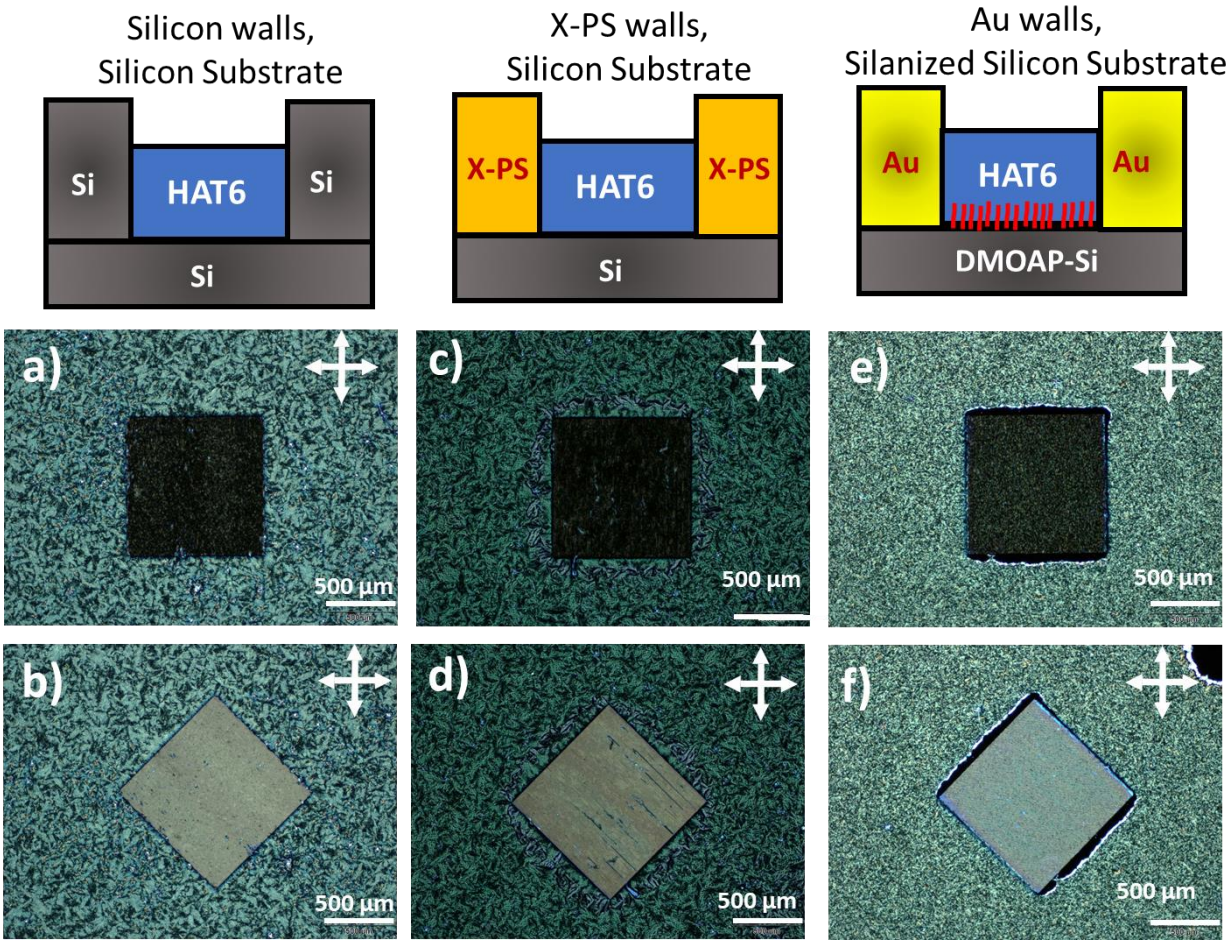

Figure S3: Influence of sidewall and substrate chemistry on optical texture. HAT6 crystals in microchannels with silicon sidewalls and substrate (a and b), X-PS side walls and silicon substrate (c and d) and gold sidewalls and silanized silicon substrate (e and f). Images are taken with the grating parallel (a

,c, and e) and rotated 45° (b,d, and f) with respect to crossed polarizers. The channel width and pitch are ≈ 3 μm and ≈ 5 μm, respectively. The thicknesses of the films are 130 to 140 nm.

The anisotropy factor, $\frac{I(45)-I(0)}{I(45)+I(0)}$, for the three samples shown in **Figure S3** are calculated and reported below.

Table S1

Sample	Anisotropy factor $\frac{I(45)-I(0)}{I(45)+I(0)}$
Si Walls Si substrate	0.8
X-PS Walls Si substrate	0.84
Au Walls DMOAP Si substrate	0.72

We attribute the small differences in the anisotropy factor to variations inherent to our sample preparation protocol. Different samples grown using the same procedure on microchannels of fixed chemistry and geometry produce the same level of variation as seen in **Table S1** (see error bars in **Figure 4** of main manuscript).

iv. Alignment in ≈ 8 μm wide channels

The degree of biaxial alignment in ≈ 8 μm wide channels is evaluated in the POM images shown below.

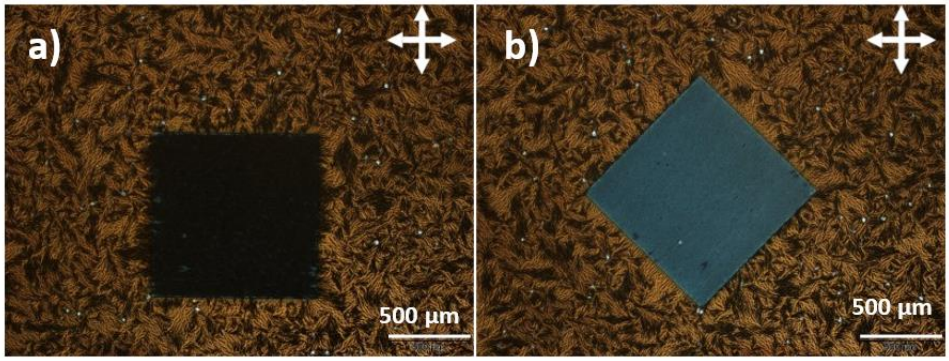

Figure S4: HAT6 crystals in ≈ 8 μm wide channels. The channel walls are made of X-PS. Images are taken with channels a) along and b) 45° to crossed polarizers.

v. Characterization of scattering from columnar peaks

Shown below is intensity as a function of the azimuthal angle χ for the peak Q ≈ 0.35 $Å^{-1}$. The peak corresponds to the spacing between the columns in the liquid crystalline phase.

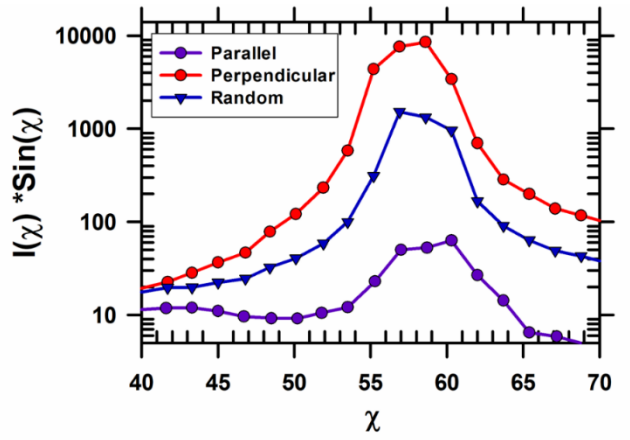

Figure S5: Sine-corrected angular intensity profiles for the peak at Q ≈ 0.35 Å^{-1}. The peak corresponds to the spacing between the columns in the liquid crystalline phase. GIWAXS patterns are collected for HAT6 in its liquid crystalline state on un-patterned silicon (blue-triangles) and in the microchannels with the X-ray beam parallel (pink circles) and perpendicular (red circles) to the X-PS gratings.

vi. Quantification of optical anisotropy in liquid crystalline and crystalline states

HAT6 films in microchannels are imaged at 80 °C and 25 °C to evaluate anisotropy in the liquid crystalline and crystalline states, respectively. Shown in **Figure S6** are images taken at these states; the sample is rotated to evaluate the degree of in-plane anisotropy. The POM images are integrated to produce the intensity profiles plotted in **Figure S6e**, which in turn are used to evaluate the anisotropy factors reported in **Table S2.** The degree of anisotropy in the liquid crystalline state is slightly lower. At higher temperatures, thermal fluctuations diminish molecule ordering to a greater extent. We attribute the slightly reduced anisotropy factor in the LC state to temperature induced disordering.

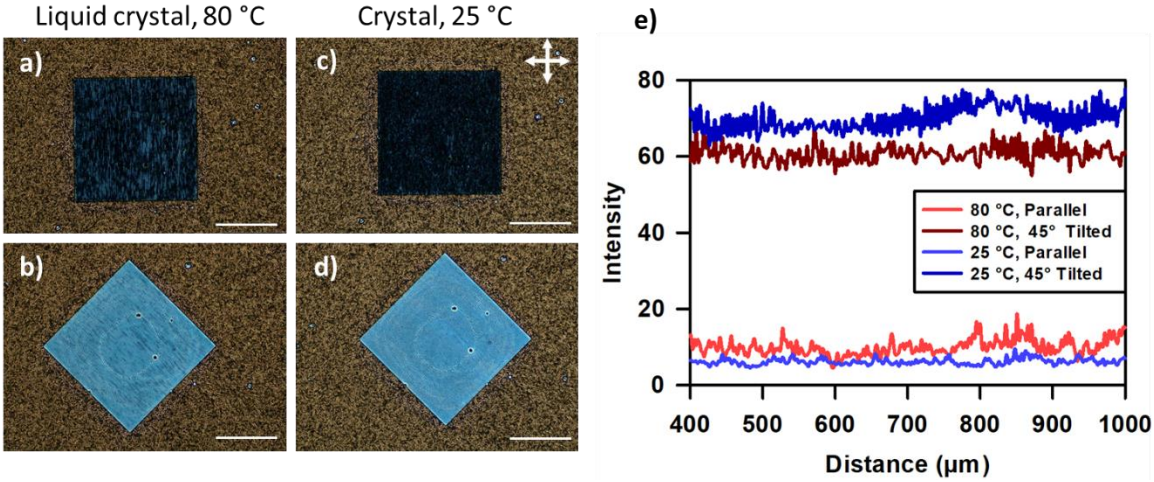

Figure S6: Polarized optical microscopy of HAT6 in microchannels in its liquid crystal (a-b) and crystal states (c-d). Images are collected with the channels parallel (a,c) and rotated 45° (b,d) with respect to the cross polarizers. The patterned regions in images a-d are integrated to produce the plot of intensity vs distance (e) . The channel width and pitch are ≈ 3 μm and ≈ 5 μm, respectively. Scale bar, 500 μm. The thickness of the HAT6 film and X-PS grating are ≈ 70 nm and ≈ 75 nm, respectively.

Table S2

Sample	Anisotropy factor $\frac{I(45)-I(0)}{I(45)+I(0)}$
Crystal, 25 °C	0.84
Liquid crystal, 80 °C	0.72

vii. Influence of thermal processing on optical texture

To determine the influence of thermal processing on optical anisotropy, thin crystalline films of HAT6 are prepared from quenching and slow cooling (1 °C/Min). POM images of crystalline HAT6 thin films varying only in thermal history are shown below in **Figure S7**. Images are collected with the gratings parallel and rotated 45° with respect to the cross-polarizers. The difference in intensity for these geometries is a measure of biaxial anisotropy. The images are integrated and plotted below the POM images for quantitative comparison of optical anisotropy. Both sets of images are acquired upon cooling from the liquid crystalline phase.

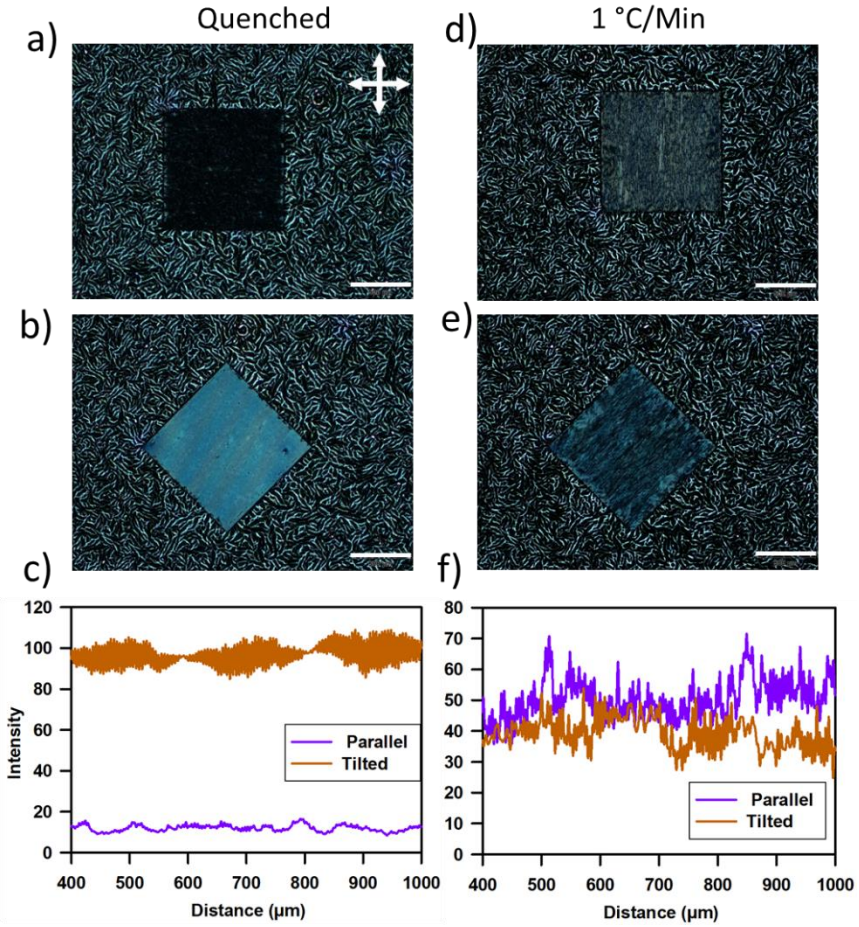

Figure S7: Dependence of optical texture on thermal history. Polarized optical microscopy of HAT6 in its crystalline state after quenching (a-c) and cooling at 1 °C/Min (d-f) from the liquid crystalline state. POM

images (a,b,d,e) are integrated to produced corresponding intensity profiles (c,f). Scale bar, 500 μm. The channel width and pitch are ≈ 3 μm and ≈ 5 μm, respectively. The thickness of the HAT6 film and X-PS grating are ≈ 70 nm and ≈ 75 nm, respectively. The difference in intensity for images collected with the gratings parallel (a,d) and tilted 45°(b,e) with respect to cross-polarizers is a measure of in-plane anisotropy. Quenching produces highly anisotropic samples whereas slow cooling produces crystalline films that are nearly isotropic in-plane.

The anisotropy factors for HAT6 films in microchannels prepared through quenching and slow cooling are reported below.

Table S3

Sample	Anisotropy factor $\frac{I(45)-I(0)}{I(45)+I(0)}$
Quenched	0.78
Slowly cooled	-0.12

We speculate that a rapid quench freezes in the lattice orientation wherein molecular organization most closely resembles that in the liquid crystalline phase. Slow cooling however results in a lattice orientation which minimizes total free energy.

viii. Images of X-PS gratings before filling

Optical and SEM images of X-PS microchannels before filling are shown below. The optical and SEM images provide top and cross-sectional views, respectively. The pitch and width of the imaged sample are 5 μm and 3 μm, respectively.

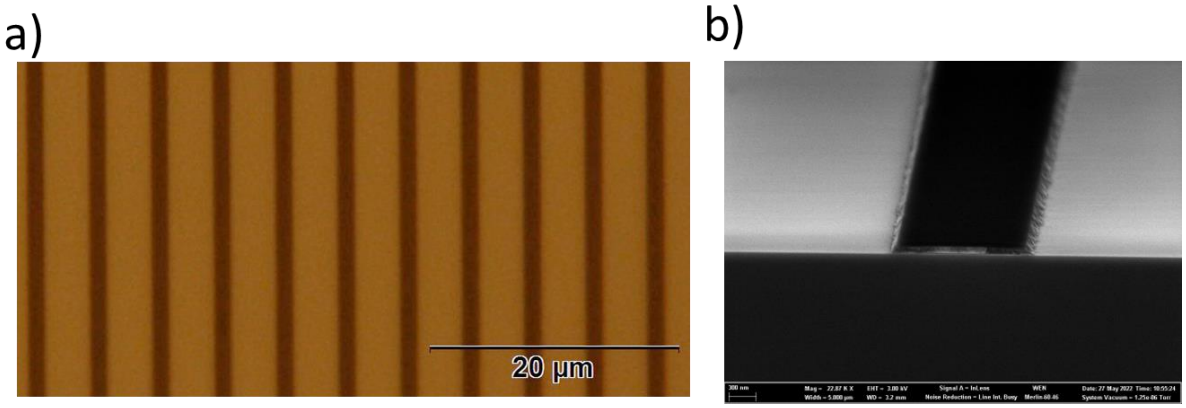

Figure S8: Microchannels for alignment of HAT6. a) Optical image and b) scanning electron micrograph of microchannels.

ix. Structure of thin films of non-mesogenic molecule, TP6EO2M, in microchannels

To study the texture of crystals of a non-mesogenic molecule in microchannels, we synthesized TP6EO2M, a molecule that closely resembles HAT6 but does not exhibit thermotropic liquid crystalline phases[1]. The molecular structure of TP6EO2M is shown in **Figure S9d**. We followed a protocol previously developed in the literature to synthesize TP6EO2M[2]. We spin-coated TP6EO2M into microchannels and quenched from 60 °C, where it is an isotropic liquid to room temperature, where it is a crystal[1]. We performed optical microscopy of the sample as shown in **Figure S9**. The POM images and the integrated intensity profiles indicate no change in intensity with in-plane rotation. Our results indicate that biaxial alignment in microchannels cannot be attained without an intermediate liquid crystalline phase between the isotropic and crystalline states.

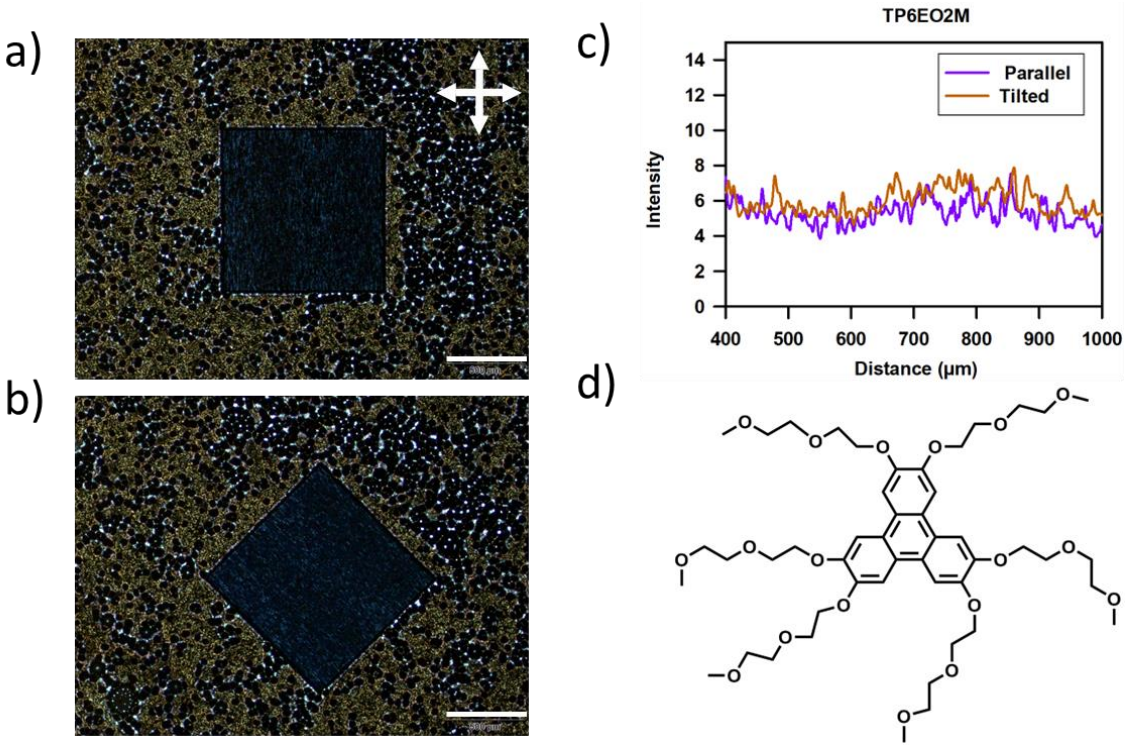

Figure S9: Structure of thin films of non-mesogenic molecule TP6EO2M in microchannels. Polarized optical microscopy images with the channels a) parallel and b) rotated 45° with respect to cross polarizers. c) Integrated intensity profiles of the patterned region in a) and b). d) Molecular structure of non-mesogenic molecule TP6EO2M. The channel width and pitch are ≈ 3 μm and 5 μm, respectively. The thickness of the film and X-PS grating are ≈55 nm and ≈ 75 nm, respectively. The POM images and intensity profiles indicate the TP6EO2M crystals exhibit in-plane isotropy in the microchannels.

References:

1 N. Boden, R. J. Bushby, Z. Lu and O. R. Lozman, *Liq. Cryst.*, 2001, **28**, 657–661.

2 R. C. Borner, N. Boden, R. J. Bushby, R. C. Borner, A. N. Cammidge, R. J. Bushby, A. N. Cammidge and M. V Jesudason, *Liq. Cryst.*, 2006, **33**, 1439–1448.